Multiscale and Multidisciplinary Modeling, Experiments and Design

Blast wave interaction with structures -- an application of exploding wire experiments

--Manuscript Draft--

Manuscript Number:	MMED-D-20-00018R1
Full Title:	Blast wave interaction with structures -- an application of exploding wire experiments
Article Type:	Original Paper
Funding Information:	National Science Foundation (CBET-1803592) — Prof. Veronica Eliasson Air Force Research Laboratory (FA8651-17-1-004) — Prof. Veronica Eliasson
Abstract:	The purpose of this research study is to build upon prior shock dynamics research to create an improved experimental setup that can be used to better understand the interaction of shock waves with structures. Large-scale blast wave experiments pose a risk to the individuals running the experiments, the surroundings, and the institution funding them. In contrast, small-scale blast experiments are able to decrease the danger and amount of funding needed associated with each experiment while producing valuable data. Simulations of blast wave-structure interaction may, on the other hand, result in extensive computational times and results that need verification. The exploding wire setup used in this research study has been optimized to consistently produce results at a run-time of less than 100 seconds per experiment. The adaptable exploding wire setup has a discharge voltage range of 10 kV - 40 kV. The configuration includes three main components: the driver, the experimental apparatus, and an ultra high-speed imaging system. The original make-up of the exploding wire apparatus allows for flexible adjustments of specifications such as initial detonation, shock wave origin, and magnitude in two and three dimensions. A recent advancement in algorithm tracking has allowed for automated detection of the individual shock fronts. In this instance, the exploding wire apparatus was adapted to simulate city-scale explosions in two dimensions, and the results were compared with numerical simulations.
Corresponding Author:	Veronica Eliasson University of California San Diego UNITED STATES
Corresponding Author Secondary Information:	
Corresponding Author's Institution:	University of California San Diego
Corresponding Author's Secondary Institution:	
First Author:	Janelle Coleen Dela Cueva
First Author Secondary Information:	
Order of Authors:	Janelle Coleen Dela Cueva Lingzhi Zheng Barry Lawlor Kevin Nguyen Alexander Westra Jorge Nunez Jane Zanteson Claire McGuire, BS Rodrigo Chavez, MSc Benjamin J Katko, BS

	Heng Liu, MSc
	Veronica Eliasson
Order of Authors Secondary Information:	
Author Comments:	
Response to Reviewers:	Response to reviewers We want to thank both reviewers for taking the time to carefully read through our manuscript and providing thoughtful comments. Comments to the author: Reviewer #1: Overall this paper presents some very interesting and relevant experiments and computational work. The work is extremely well done and contains a lot of detailed insights that are important to be discussed. 1) How were the size and orientation of the buildings chosen page 6 line 10-12 The size of the buildings were chosen to best fit into the viewing area of the experimental schlieren system, while also allow for the structures to be printed by a tabletop 3-D printer. The relative orientation of the buildings were chosen such that the walls of the buildings were all parallel to each other to simulate a street environment. The buildings were positioned such that the walls are 45 degrees from the vertical axis to observe oblique impacts of the incident shock. Specific orientations and placements of the structures are explained on Page 6, line 4. The structure dimensions were determined to best fit into the viewing area of the experimental schlieren system, while also allow for the structures to be printed by a tabletop 3-D printer. The relative orientation of the buildings were chosen such that the walls of the structures were all parallel to each other, simulating a street environment. The structures were positioned such that the walls are 45 degrees from the vertical axis to observe oblique impacts of the incident shock. 2) Did you perform any calibrations without obstacles to prove the assumptions in page 7 line 6-8 are valid for your setup and scaling. This seems like it would help eliminate any difference early on. As mentioned on page Page 7, line 11:, though not explicitly, the blast initial conditions using Taylor's similarity law was verified in Qiu and Eliasson's 2015 paper, where the pressure history obtained from Overture at a given location away from the blast center was compared to a micro-scale experiment, and the simulated results agreed well with the experimental ones. Page 7, line 11: The equilibrium equations were simplified to two-dimensional form (Shaolin 1954), and have previously been used with Overture by Qiu and Eliasson (Qiu 2015) where the pressure history obtained from Overture at a given location away from the blast center was compared to a micro-scale experiment, and the simulated results agreed well with the experimental ones. 3) The plots in figure 6 show your density results are dependent on the grid size. They seem to converge as you get smaller. However it says nothing about the reflected waves, is there a fuller visual comparisons you can do to show you get similar front propagation especially after complex interactions. The manuscript has been updated accordingly. Page 8, line 25: The incident wave occurs at an oblique angle to Structures A and B, resulting in the initial density peaks shown in Fig. 6 at approximately 13 us. The subsequent larger peaks are due to shock reflections caused by the presence of structures A and B, and shock interactions. Also: Line style for legends for the 1/25 mm grid has been added in Figure 6. 4) Figure 7, can you subtract the two images to see where the two fronts differ. This seems like it would highlight the variations quickly. This is a good idea. However, we tried superimposing the images on top of each other using different approaches and the result was not very good. We need to think more about this and can certainly incorporate it in our future work. 5) Figure 7 is the experiment having a harder time picking up the secondary waves due to the limited resolution of the camera?

	The manuscript has been updated accordingly. Page 9, line 9: It should be noted that the lack of secondary, tertiary etc. shocks in the experimental photographs is not only due to camera resolution but also because these shocks are not strong enough to be clearly visualized by the current schlieren imaging setup. If the initial explosion was stronger, these waves would be easier to visualize. 6) Figures 8 and 9 needs units on the pressure. The manuscript has been updated accordingly. Page 9, line 15: The pressure values have been nondimensionalized using Eqn. (3) shown earlier. Figure 8 caption has been updated accordingly: Nondimensionalized pressure contours at two time instants showing the resulting blast wave impact onto structures A and B Figure 9 caption has been updated accordingly: Nondimensionalized pressure contours at two later time instants showing the resulting blast wave impact onto all structures and the resulting shock-shock interaction in between the buildings. 7) The last sentence of page 9 line 18 is really important. Is there something you can learn about building spacing, orientation etc to minimize this? From Heng: Should say something more about what we learned from the numerical & experimental results. Page 10, line 2: Moreover, stronger shock focusing seems to occur adjacent to more densely spaced structures. However, future careful parametric studies on e.g. building spacing and orientations need to be conducted to determine the exact configurations that minimize blast damage. Reviewer #2: The authors conducted both experimental and numerical studies to investigate the interaction of shock wave and multiple structures. The paper is interesting and was well presented. Before publication, the paper needs to address some clarifications as stated below: * The dimensions stated in page 6 (line #9 - 12) do not seem to correlate to the sizes sketched in Figures 3 and 4 at least qualitatively. For example, Structure E is 26 mm x 13 mm, which is the smallest among all in terms of the given dimensions. However, it looks the largest in the figures. The dimensions have been corrected. Page 6, line 15: The dimensions for structure A are 37.5 mm × 27.5 mm, structure B are 26 mm x 13 mm, structure C are 37.5 mm × 27.5 mm, structure D are 26 mm x 13 mm, and structure E are 100 mm × 50 mm. * In Figure 7, which one is the experimental measurement, and which one is the numerical result? Since a one-fifth model was used for the numerical study, was the numerical result enlarged for the comparison. For all (a), (b), (c) and (d), the image to the left is the experimental result and the image on the right is the result from the simulation. The manuscript has been updated accordingly. Page 18, line 27: Fig. 7: Comparison of experimental (left) and numerical (right) schlieren results: (a) t = 16 μs, (b) t = 23 μs, (c) t = 31 μs,and (d) t = 38 μs. * When the structural size was scaled by one-fifth, what about the thickness of the structure? Was the structure assumed rigid? Correct, for these simulations the structures are assumed to be rigid. See Page 7, line 20. * Why did they use the scale down model for the numerical study? Can they use the same dimensions as in the experimental set-up while increasing the mesh size and the time step size? We did perform a full scale simulation, however, not at the finest grid resolution that we used for the smaller scale model. This simulation took a really long time, and due to limited computational resources we simply could not perform the full-scale, fine-grid simulation. We compared the result of the course grid full scale simulation with the outcome of the scaled-down simulation. We observed very similar shock patterns from the full scale

	and the scaled-down simulations. Hence, we concluded that it is ok to use the smaller scale simulation, whose smaller size allowed us to implement more refined grid size, for comparison with the experiments. Page 7, line 27: A full scale simulation using a coarse grid was performed to validate the qualitative features of the scaled-down simulations. The grid used in the full scale simulation contained the same amount of grid lines as that used in the scaled-down simulation. The shock pattern yielded from the full scale simulation is qualitatively similar to that from the scaled-down simulation. It was also clear that even with a coarse grid, the computational time and data storage costs of a full scale simulation surpassed those from the scaled-down simulation by a significant margin, and it proved to be impossible at this time to run the full scale simulation at the finest grid resolution due to lack of computational resources. Hence, a scaled-down simulation was chosen for comparison with the experiments. Reflecting on the cost of a full scale simulation further shows the advantage of the exploding wire experimental setup. * How did they model the exploding wire? Is there any empirical expression for the shock pressure? The wire explosion process is not simulated, instead, we focus on the propagation of the resulting blast wave after the wire has exploded. As mentioned in the manuscript, the spatial pressure distribution can be predicted using Taylor's similarity law. Page 7, line 9: The physical and chemical processes of the wire explosion were not simulated, instead, the gas properties behind the blast front resulting from the wire explosion were estimated by Taylor’s similarity law (Taylor (1950)). * Can the author measure the pressure and compare the experimental and numerical pressure? This is a very good idea, and something we have in mind for future work on this setup. The manuscript has been updated accordingly. Page 10, line 20: Pressure measurements for the experiments will be incorporated in future experiments, with the minimal drawback of blocking part of the optical path of the schlieren system where the pressure sensors are installed.

Noname manuscript No.
(will be inserted by the editor)

Blast wave interaction with structures – an application of exploding wire experiments

Janelle Coleen Dela Cueva[1] · Lingzhi Zheng[2] · Barry Lawlor[2] · Kevin Nguyen[1] · Alexander Westra[1] · Jorge Nunez[2] · Jane Zanteson[1] · Claire McGuire[2] · Rodrigo Chavez[1] · Benjamin J Katko[1] · Heng Liu[1] · Veronica Eliasson[1*]

Received: date / Accepted: date

Abstract The purpose of this research study is to build upon prior shock dynamics research to create an improved experimental setup that can be used to better understand the interaction of shock waves with structures. Large-scale blast wave experiments pose a risk to the individuals running the experiments, the surroundings, and the institution funding them. In contrast, small-scale blast experiments are able to decrease the danger and amount of funding needed associated with each experiment while producing valuable data. Simulations of blast wave-structure interaction may, on the other hand, result in

This study was supported by the US Air Force Research Laboratory under grant No. FA8651-17-1-004 and the National Science Foundation under grant number CBET-1803592.

[1]Department of Structural Engineering
University of California, San Diego,
La Jolla, CA 92093-0085, USA
E-mail: rchavezm@eng.ucsd.edu
E-mail: bkatko@eng.ucsd.edu
E-mail: hel108@eng.ucsd.edu
E-mail: awestra@ucsd.edu
E-mail: ktn105@ucsd.edu
E-mail: jcdelacu@ucsd.edu
E-mail: jzanteso@ucsd.edu
V. Eliasson
E-mail: eliasson@ucsd.edu
Phone: +1 858 534 5928
ORCID: 0000-0001-5134-1399
[2]Department of Mechanical and Aerospace Engineering
University of California, San Diego,
La Jolla, CA 92093-0085, USA
E-mail: jln018@ucsd.edu
E-mail: liz147@ucsd.edu
E-mail: blawlor@ucsd.edu
E-mail: c1mcguir@ucsd.edu

extensive computational times and results that need verification. The exploding wire setup used in this research study has been optimized to consistently produce results at a run-time of less than 100 seconds per experiment. The adaptable exploding wire setup has a discharge voltage range of 10 kV – 40 kV. The configuration includes three main components: the driver, the experimental apparatus, and an ultra high-speed imaging system. The original make-up of the exploding wire apparatus allows for flexible adjustments of specifications such as initial detonation, shock wave origin, and magnitude in two and three dimensions. A recent advancement in algorithm tracking has allowed for automated detection of the individual shock fronts. In this instance, the exploding wire apparatus was adapted to simulate city-scale explosions in two dimensions, and the results were compared with numerical simulations.

Keywords Shock dynamics · Shock-structure interaction · Schlieren photography · Exploding wire · Blast wave

1 Introduction

Experimental blast wave research has proven valuable when studying how standing structures interact with blast wave loading. Blast wave experimental research has been performed to study how blast waves propagate in urban environments (Fouchier et al., 2017; Smith and Rose, 2006; Rose et al., 2006). However, given the destructive nature of blast waves, performing a single full-scale experiment requires a tremendous concern for safety due to the use of explosives. The destructive nature of an explosive event can also limit the amount of data acquired during the experiment. An alternative method relies on computational research, such as the studies performed by Togashi et al. (2010) and Valger et al. (2017). However, given the complex nature of the fluid dynamics involved in fluid-solid interactions, reliable experimental studies are still necessary to confirm the physical results that are being simulated.

Some of the main drawbacks that come with experiments involving chemical explosives have been observed by Held (1999). The fireball created by the explosion in Held's study makes it nearly impossible to obtain adequate measurements in the vicinity of the charge during the experiment. Furthermore, such experiments may come with a high cost as demonstrated by Smith and Rose (2006), where city scale models constructed with concrete and steel were destroyed by the subsequent explosion, making it extremely cumbersome to perform repeatable studies.

Hosseini and Takayama (1999) used a different setup in which exploding silver azide pellets were used to generate spherical shock waves inside a spherically shaped cavity. However, this setup included a nonuniform shock front and indentations on the transparent portion of their test section due to silver azide pellet fragments traveling ahead of the shock front and impacting the test section walls.

The exploding wire concept has been used to study gas dynamics events ever since Ernst Mach used two exploding wires to study shock wave reflections

in the 1870s (Blackmore (1972)). The exploding wire setup used in this present study was first introduced by Lakhani (2018), and further expanded by Mellor et al. (2019), and it has been enhanced for use in this present research study because it presents solutions to the issues aforementioned. The setup does not rely on chemical explosives, but on thin copper wires that are charged with a high electric potential causing them to turn into plasma through ohmic heating, and the resulting explosion creates a blast wave that can be used to study blast-structure interaction. This arrangement poses minimal risk to the users due to the less volatile nature of the explosion. Moreover, the exploding wires can be placed in interchangeable experimental arrangements depending on the study of interest. The portability and adaptability of the exploding wire setup allows the experiments to be safely conducted in a laboratory setting with no need for outdoor experiments. Experimental arrangements with 3-D printed parts used as structures has the benefit of achieving easily customizable shapes, with the main limitation of this arrangement being the construction of new obstacles – nevertheless, the 3-D printing technique is more versatile and faster than casting concrete structures (Smith and Rose (2006)).

In this study, the exploding wire setup was used to perform high-fidelity small-scale city landscape-blast experiments. The experiments presented here have a turnaround time between consecutive experiments of approximately 100 seconds, and thus lend the ability to perform several dozens of experiments in any given day at a very low cost.

In this study, a 2-D blast wave setup was utilized. One exploding wire was placed in between two thin Poly(methyl methacrylate) (PMMA) optically transparent sheets. Rectangular 3-D printed obstacles were secured between the sheets and around the exploding wire to simulate buildings in a cityscape. Upon explosion, a blast wave propagated towards the obstacles, resulting in multiple shock reflections and interactions. Schlieren photography was used in conjunction with ultra high-speed photography to visualize the blast phenomenon, allowing full visualization of the different interactions occurring during the experiment.

Furthermore, numerical simulations of the same setup were performed using Overture, a numerical solver where the Euler equations of gas dynamics are solved on overlapping grids. Good agreement between the experiments and simulations was observed. It is interesting to note that in this case, the exploding wire setup can produce large datasets of results much faster than the numerical simulations. The computational cost of the simulations is high and thus requires a significant amount of time and storage.

2 Exploding wire setup

The exploding wire setup design has been explained in detail by Mellor et al. (2019) and only a brief introduction will be presented herein. The exploding wire setup consists of three primary subsystems: (1) driver, (2) experimental test section, and (3) ultra-high-speed imaging system. The driver, Fig. 1,

stores the desired charge in several capacitor banks and discharges the current through a spark gap and outlet leads. Once discharged, the current travels to the experimental apparatus and the test section where the thin copper wire is heated rapidly, thus resulting in plasma generation, and once it expands a shock front is created. Finally, the imaging system captures the experiment through a series of ultra high-speed photographs that allow for quantitative analysis of the shock dynamics event.

The setup was designed with the ability to carefully tune the system for the desired voltage output, allowing for a wide range of experimental settings to be explored. With an experimental turnaround time of approximately 100 seconds, the system allows for rapid data extraction. For safety purposes, the system was built with multiple automatic grounding safeguards in place. Finally, the exploding wire setup is manually grounded after each experiment to further ensure safety. The circuitry of the exploding wire system is shown in detail in Fig. 2.

2.1 Driver system

The driver subsystem was constructed of a capacitor bank consisting of four individual capacitors (0.22 μF, General Atomics, Part No. 31160) connected in parallel that store up to 50 kV each; two electromagnetic switches (Ross Engineering, Model No. E40-DT-60) that control the charging circuit and the grounding circuit; a spark gap (10-65 kV, Hofstra Group, Item No. 3114), which opens and closes the discharging circuit; and a Rogowski coil (Pearson Electronics) that triggers the camera to record images. This configuration is shown in Fig. 1.

The voltage source, in conjunction with the switches, applies voltages ranging from 10 kV to 40 kV to the capacitor bank. After storage, the spark gap is triggered pneumatically using a roughing pump. The air pressure in the spark gap is reduced such that the air dielectric constant reaches the self-breakdown point, at which point the discharging circuit is completed. With a closed circuit, the current exits the capacitor bank, traveling through an outlet lead to the experimental test section, where it produces the ensuing shock wave. The discharge circuit is also equipped with a Rogowski coil connected to an oscilloscope (Picoscope 4824). When the current discharges, the signal from the Rogowski coil, which is monitored by the oscilloscope, is used to trigger the high-speed camera to begin recording photographs of the resulting blast event.

2.2 Experimental apparatus

The experimental test section apparatus is an interchangeable structure in which the explosion event occurs. As shown in Fig. 3, consistent in each apparatus is the use of two brass electrodes set 25.4 mm (1 in) apart, with an exploding copper wire strung across the electrodes. The outlet lead is connected

to both electrodes, with the hot wire connected to one of the electrodes and the ground connected to the other electrode. When the discharge of current occurs, the current short-circuits through the thin copper wire, resulting in ohmic heating. Thus, the solid copper instantly turns into plasma that subsequently disperses explosively, and the shock wave is created, and its interaction with the structures is captured via the ultra high-speed camera system.

2.3 Ultra high-speed imaging setup

A z-folded schlieren configuration was used to visualize the propagating blast waves. A razor blade was used as a schlieren edge to visualize the shock fronts by filtering the refracted light rays that had passed through regions of differing density gradients.

A Shimadzu HPV-X2 ultra high-speed camera was used to record the shock wave propagation across the cityscape at 500,000 fps. The blast phenomenon was captured using 256 frames at a resolution of 250 pixels $\times$ 400 pixels. A light emitting diode was used to illuminate the 127 mm $\times$ 200 mm (5 in $\times$ 8 in) elliptical field of view. Due to the inherent geometrical limitations of a z-folded schlieren setup, the field of view is confined to an elliptical shape that may restrict the amount of data a user can gather from the event of interest, depending on the aspect ratio of the imaging device. To alleviate this issue, a dove prism was introduced to simply turn the orientation of the schlieren field of view by 90° to maximize the viewing region of the experiment by aligning it to the camera's sensor.

3 Small-scale experiments simulating a cityscape

The exploding wire setup is adaptable to small-scale experiments simulating blast waves propagating through a cityscape. The 3-D printed objects were modeled as cityscape structures with the purpose of investigating the shock behavior and interaction between structures as seen from a bird's-eye view, featuring a 2-D setup. The structures were printed with smooth surfaces to prevent shock waves from causing disturbances when reflecting off the walls. The 2-D cityscape test section in Fig. 3 was constructed with 80/20 t-slot aluminum profiles for flexible customizability of the experimental configuration. Two 6.35 mm (0.25 in) thick PMMA panels were placed between the t-slots to accommodate the 3-D printed structures. Holes with diameters of 25.4 mm (1.0 in) were laser cut into the 508 mm $\times$ 508 mm (20 in $\times$ 20 in) acrylic plates to hold the two brass electrodes, such that a 0.05 mm (0.002 in) diameter and 50.8 mm (2 in) long copper wire could be draped across both electrodes. For stability, lead weights were attached on either ends of each copper wire.

The cylindrically propagating blast wave interacts with five obstacles, structures A through E in Fig. 3 and Fig. 4, of a fixed out-of-plane depth of 25.4 mm (1 in). The black dashed lines enclosing the white area in Fig. 4 denote the

boundaries of the camera's viewing area of the experiment. The red circle in Fig. 4 identifies the source of the blast wave. The structures were sandwiched between the PMMA panels at predetermined positions with small amounts of putty used for adhesion and rigidity. The structure dimensions were determined to best fit into the viewing area of the experimental schlieren system, while also allow for the structures to be printed by a tabletop 3-D printer. The relative orientation of the buildings were chosen such that the walls of the structures were all parallel to each other, simulating a street environment. The structures were positioned such that the walls are 45° from the vertical axis to observe oblique impacts of the incident shock. Structures A and B were oriented to focus the shock wave downstream. Structure C was placed such that a reflected wave impacts the side of the wall. Structure D was placed to observe the impact of a reflected wave on a corner of a structure. Finally, structure E was positioned to observe the interaction from the Mach stem as it propagates along an extended surface. The dimensions for structure A are 37.5 mm × 27.5 mm, structure B are 26 mm × 13 mm, structure C are 37.5 mm × 27.5 mm, structure D are 26 mm × 13 mm, and structure E are 100 mm × 50 mm.

The schlieren photographs of the blast wave propagation through the cityscape setup were processed to obtain automated tracking of the incident and reflected shock fronts. The tracking was performed using a series of algorithms carefully explained in the previous work by Zheng et al. (2020). In short, a reference grid was used to correct the optical distortions inherent to the z-folded schlieren setup. The background from an initial photograph (obtained before the shock wave enters the field of view) was then subtracted from all subsequent schlieren photographs to isolate the shock fronts in the form of binary pixels. Morphological operations were utilized to highlight the shock fronts while eliminating noise. Individual shock fronts were then identified from the entangled shock fronts and separately tracked with a discretization algorithm.

4 Numerical simulations

The Overture software package, a free software that can be downloaded online (https://www.overtureframework.org/ (2012)), was used to simulate the cityscape experiment above. The Euler equations of conservation of mass, conservation of momentum, and conservation of energy were solved using the second-order Godunov method (Henshaw and Schwendeman (2003, 2006)). The grid for the structures' geometry was constructed with overlapping grids using the grid generator included in the Overture software package.

The initial conditions in front of the blast waves were set to be those of ambient air at $p_0 = 101,325$ Pa and of room temperature at $T_0 = 294$ K. The specific heat ratio of air was $\gamma = 1.4$, and the specific gas constant of air was $R_g = 287$ J/(kg·K). The ideal gas law was used for the equation of state. The energy density of the point-blast source in 2-D was estimated to be 300 J/m,

and the radius of initial blast was set to be 0.5 mm. Density, velocity, pressure, time, and distance were non-dimensionalized as shown in equations 1 to 5:

$$\rho* = \rho/\rho_0, \tag{1}$$

$$u* = u/\sqrt{\gamma R_g T_0}, \tag{2}$$

$$p* = p/(\rho_0 \gamma R_g T_0), \tag{3}$$

$$t* = t/(L_0/\sqrt{\gamma R_g T_0}), \tag{4}$$

$$L* = L/L_0, \tag{5}$$

where $\rho_0 = 1$ kg/m^3, and $L_0 = 1 \cdot 10^{-3}$ m.

The physical and chemical processes of the wire explosion were not simulated, instead, the gas properties behind the blast front resulting from the wire explosion were estimated by Taylor's similarity law (Taylor (1950)). The equilibrium equations were simplified to two-dimensional form (Shao-Lin (1954)), and have previously been used with Overture by Qiu and Eliasson (Qiu and Eliasson (2015)) where the pressure history obtained from Overture at a given location away from the blast center was compared to a micro-scale experiment, and the simulated results agreed well with the experimental ones. In the current study, the two-dimensional form of Taylor's similarity law was used to provide initial conditions behind the blast front for the subsequent cityscape simulations.

The structures in the cityscape were modeled as rigid obstacles with slip walls. Annular overlapping grids formed around the structures were used to exchange information with the square background grid. As shown in Fig. 5(a), structures A through E are surrounded by annular grids, and in Fig. 5(b), overlapping grids between the structure and the background are shown.

The size of the computational domain was chosen to be 31 mm × 50 mm, and therefore the obstacles were scaled-down to be five times smaller than the structures from the experimental setup. A full scale simulation using a coarse grid was performed to validate the qualitative features of the scaled-down simulations. The grid used in the full scale simulation contained the same amount of grid lines as that used in the scaled-down simulation. The shock pattern yielded from the full scale simulation is qualitatively similar to that from the scaled-down simulation. It was also clear that even with a coarse grid, the computational time and data storage costs of a full scale simulation surpassed those from the scaled-down simulation by a significant margin, and it proved to be impossible at this time to run the full scale simulation at the finest grid resolution due to lack of computational resources. Hence, a scaled-down simulation was chosen for comparison with the experiments. Reflecting on the cost of a full scale simulation further shows the advantage of the exploding wire experimental setup. The total thickness of the obstacle grids is defined as the normal distance from the outermost layer of the annular grids to the obstacle surface and is fixed to 0.5 mm. The size of the annular grids is uneven in such a way that the closer a layer of grid cells is to the obstacle surface, the more refined it is, as indicated in Fig. 5(b). The cell sizes of the annular obstacle

grids as well as the square background grids were chosen after performing a grid convergence study. To define an obstacle in Overture, coordinates of obstacle corners are required, then the innermost layer of annular grids that contours the obstacle would be automatically generated through a built-in interpolation function. It is worth noting that the roundness of obstacle corners can be controlled by the user through the function shown in equation (6), where coefficients d_j and f_j are defined by the input vertices (Henshaw (2011a)). For this study, the non-dimensional corner sharpness coefficient, e_j, was chosen to be 90 to be as consistent with the experimental setup as possible.

$$V_j(x) = \frac{d_j - 1}{2} \log\left(\frac{\cosh e_j(x - f_j)}{\cosh e_j(x - f_{j+1})}\right)\frac{1}{2e_j} \tag{6}$$

A grid convergence study was performed in which identical simulations were carried out on square background grids with grid cell sizes varying from 1/8 mm to 1/25 mm. Though the size of the annular grid cells is not the same in the radial direction, the number of annular grid cells increased by the same ratio as the refinement of the background grid. The density of the flow was probed at two locations, as shown in Fig. 4. Probe 1 (P1 in Fig. 4) was placed on the background grid between the obstacles to test the effectiveness of the background grid density as well as the interaction between the background and annular grids. Probe 2 (P2 in Fig. 4) was placed on the annular grid neighboring structure B to monitor the effectiveness of the annular grid density. The outcome of the grid convergence study is shown in Fig. 6(a) and (b). The results from the 1/20 mm grid and the 1/25 mm grid displayed a density difference of 0.44% at Probe 1 and 1.14% at Probe 2. This outcome shows that the grid size of 1/25 mm is satisfactory for the purpose of this study. The incident wave occurs at an oblique angle to Structures A and B, resulting in the initial density peaks shown in Fig. 6 at approximately 13 μs. The subsequent larger peaks are due to shock reflections caused by the presence of structures A and B, and shock interactions.

Overture schlieren is defined to visualize gas density gradients in the x, y and z-directions (Henshaw (2011b)). However, since these simulations were performed in 2-D, only $x-$ and $y-$ density gradients were present. The numerical schlieren definition can be expressed as follows:

$$\text{schlieren} = \alpha \exp(-\beta s(\mathbf{x})) \tag{7}$$

$$s(\mathbf{x}) = (\bar{s} - \min(\bar{s}))/(\max \bar{s} - \min \bar{s}), s \in [0, 1] \tag{8}$$

$$\bar{s}(\mathbf{x}) = \sqrt{\rho_x^2 + \rho_y^2} \tag{9}$$

Figure 7 shows a comparison between the numerical and experimental schlieren results in which individual experimental photographs most similar in wave pattern are compared to the respective numerical schlieren results. It can be seen that the experimental and numerical results agree very well, resulting in qualitatively similar wave patterns, but a closer comparison between experiment and simulations shown in Fig. 7(b) shows that the curvature of the

Mach reflection (indicated by the red circle), which is generated by the interaction of the reflected blasts diffracted by structures A and B, separately, is visually larger in the numerical simulation than in the experiment. This can be attributed to a discrepancy between the estimated energy release level in the simulations' initial conditions and the actual energy released by the exploding wire experiment. The unpredictable angle and complex nature of physical explosions pose a challenge in estimating the energy release level during the explosion, but the experiments can be used to qualitatively verify the computational results. It should be noted that the lack of secondary, tertiary etc. shocks in the experimental photographs is not only due to camera resolution but also because these shocks are not strong enough to be clearly visualized by the current schlieren imaging setup. If the initial explosion was stronger, these waves would be easier to visualize.

Pressure plots of the computational domain were also obtained to evaluate the blast wave impacts onto the structures. The pressure values have been nondimensionalized using Eqn. (3) shown earlier. A discussion of the pressure contour results may be divided into two stages corresponding to different levels of blast wave interactions in between the structures. In the initial stage, it can be seen that high-pressure zones are formed between the impacted walls of structures A and B and the reflected shock wave in the region marked as I in Fig. 8(a). A comparison between Figs. 8(a) and (b) shows that these high-pressure zones are temporarily resolved as the blast front diffracts from A and B, and continues to propagate further downstream towards buildings C, D, and E. Later, at time instant $t = 26.2$ μs, a Mach stem is forming in the center of the flow field between the open area of structures A and B. The high-pressure region, marked as region II in 8(b), is formed as this Mach stem impacts structure C and reflects off its surface.

As the blast front propagates further downstream and away from the explosive's origin, the wave patterns and pressure distributions become even more complex. Figures 9(a) and (b) show that as the blast front propagates along the wall of structure E, the maximum pressure remains at the leading edge of the blast front as indicated by region IV in Fig. 9(a), but the magnitude of this pressure reduces as time progresses. Additionally, as indicated by regions V in Fig. 9(a) and VI in Fig. 9(b), it is noticeable that the flow field in the middle region of the computational domain that is surrounded by all the structures features many smaller high-pressure zones at distances away from the structure walls. These high-pressure zones develop as a result of the focusing effect of multiple weaker reflected blast waves interacting with each other. Especially in Fig. 9(b), a cluster of smaller high-pressure zones developed similar or even higher magnitudes of pressure values when compared to region IV in Fig. 9(a). This shows that unlike the initial blast wave impacts onto structures A and B (i.e. at time instants $t = 14.5$ μs and $t = 26.2$ μs), where high-pressure zones are generated on the impacted walls at time instances after the blast initiation (i.e. $t = 34.9$ μs and $t = 43.0$ μs), high-pressure regions can emerge in between the structures. This suggests that in real-world blast events, the focusing effect due to multiple reflected blast waves can cause a second round of damage to

people and property located in between buildings following the passage of the initial blast front. Moreover, stronger shock focusing seems to occur adjacent to more densely spaced structures. However, future careful parametric studies on e.g. building spacing and orientations need to be conducted to determine the exact configurations that minimize blast damage.

5 Conclusion

The series of experiments performed in this study shows the feasibility of using a small-scale blast wave experimental setup based on the exploding wire technique. The experimental turn-around time is less than 100 seconds and coupled with ultra high-speed schlieren photography the setup can generate a large amount of data in a short time span. Results show that the initial shock wave generates a Mach stem as it propagates between structures A and B. This Mach stem then interacts with structure C and E.

The simulation results agree qualitatively with the experimental results. Pressure plots generated by the simulation results show that indeed the high-pressure regions appear on the structures as the shock is reflected and in regions with shock-shock interactions – as expected. Pressure measurements for the experiments will be incorporated in future experiments, with the minimal drawback of blocking part of the optical path of the schlieren system where the pressure sensors are installed.

It is noteworthy to discuss the advantages and disadvantages of both the experimental and numerical approaches used here. First, a comparison of resources to get results from either approach makes it clear that the experimental setup requires a larger monetary initial investment to design, obtain all parts, and construct. However, once the exploding wire setup is built and an appropriate imaging system has been acquired, the setup is ready for experimentation. The initial monetary investment in the experimental setup can be paid off over time because of the much larger amount of data that can be generated per time unit compared to that of the numerical simulations. For example, during a period of one hour, Overture produces one simulation at a grid size of eight divisions per unit length when using eight cores for the simulation, while the exploding wire experiment can produce up to 36 experiments during the same time. Additionally, the exploding wire setup can easily be accommodated into a 3-D setup to investigate spherical or elliptical shock front interactions with a cityscape. Converting the simulations into 3-D will require even more simulation time than the initial 2-D simulations.

Even so, the simulation results are useful because they provide full-field data of more flow variables than is currently possible to obtain using the existing experimental exploding wire setup, thus showing the excellent synergy of a hybrid approach relying on both experiments and simulations. Pressure sensors rated for shock loads could be added to the experimental setup to generate more data, but there is no straightforward path to obtain full-field pressure data from the experiments. Background oriented schlieren techniques

(e.g. Hargather and Settles (2007); Wang et al. (2016)) could potentially be used, keeping in mind that the limited Shimadzu camera spatial resolution will result in an even more limited resolution of the obtained pressure field.

Future plans include expanding the 2-D experimental setup to 3-D to study how the height of the structures influences the blast-structure interaction. It is imperative to understand the interaction between the ground and the height of the structures to learn where Mach stems appear, as the difference in pressure behind a Mach stem and that of an incident shock wave can result in life or death situations, depending on which floor people are on in a building. Furthermore, plans to obtain a more precise estimate of the amount of energy that is released during the exploding wire event if given the input energy to the capacitor bank, are needed. This will enable improved simulations, as one does not have to start with an educated guess of the initial energy used in the charge and then go back and forth until the computational results agree with the experimental results.

Acknowledgements The authors would like to thank the US Air Force Research Laboratory under grant No. FA8651-17-1-004 and the National Science Foundation under grant number CBET-1803592 for supporting this study. We would like to acknowledge the UC Leadership Excellence through Advanced Degrees program and the Undergraduate Research Scholarship program for their support. The Mechanical Engineering Undergraduate Machine Shop was integral in the production of experiment samples.

On behalf of all authors, the corresponding author states that there is no conflict of interest.

References

Blackmore JT (1972) Ernst Mach; his work, life, and influence. University of California Press, Los Angeles,

Fouchier C, Laboureur D, Youinou L, Lapebie E, Buchlin JM (2017) Experimental investigation of blast wave propagation in an urban environment. Journal of Loss Prevention in the Process Industries 49(Part B):248–265

Hargather MJ, Settles GS (2007) Optical measurement and scaling of blasts from gram-range explosive charges. Shock waves 17:215–223

Held M (1999) Impulse method for the blast contour of cylindrical high explosive charges. Propellants, Explosives, Pyrotechnics 24:17–26

Henshaw W (2011a) Mappings for overture a description of the mapping class and documentation for many useful mappings. Technical Report: UCRL-MA-132239, Centre for Applied Scientific Computing, Lawrence Livermore National Laboratory

Henshaw W (2011b) The plotstuff graphics post processor for overture user guide, version 1.00. Technical Report: UCRL-MA-138730, Centre for Applied Scientific Computing Lawrence Livermore National Laboratory

Henshaw W, Schwendeman D (2003) An adaptive numerical scheme for high-speed reactive flow on overlapping grids. Journal of Computational Physics 191:420–447

Henshaw W, Schwendeman D (2006) Moving overlapping grids with adaptive mesh refinement for high-speed reactive and non-reactive flow. Journal of Computational Physics 216(2):744–779

Hosseini SHR, Takayama K (1999) Implosion of a spherical shock wave reflected from a spherical wall. Journal of Fluid Mechanics 530:223–239

Overture Website, (2012): https://www.overtureframework.org/ Accessed: May 2020

Lakhani E (2018) Design of exploding wire system. Master's Thesis, University of California, San Diego

Mellor W, Lakhani E, Valenzuela JC, Lawlor B, Zanteson J, Eliasson V (2019) Design of a Multiple Exploding Wire Setup to Study Shock Wave Dynamics. Experimental Techniques pp 1–8

Qiu S, Eliasson V (2015) Interaction and coalescence of multiple simultaneous and non-simultaneous blast waves. Shock Waves pp 1–13

Rose TA, Smith PD, May JH (2006) The interaction of oblique blast waves with buildings. Shock Waves 16(1):35–44

Shao-Lin L (1954) Cylindrical shock waves produced by instantaneous energy release. Journal of Applied Physics 25(1):54–57

Smith PD, Rose TA (2006) Blast wave propagation in city streets—an overview. Progress in Structural Engineering and Materials 8(1):16–28

Taylor G (1950) The formation of a blast wave by a very intense explosion. i. theoretical discussion. In: Proceedings of the Royal Society 684 of London Series A Mathematical and Physical Sciences pp 159–174

Togashi F, Baum JD, Mestreau E, Löhner R, Sunshine D (2010) Numerical simulation of long-duration blast wave evolution in confined facilities. Shock Waves 20(5):409–424

Valger SA, Fedorova NN, Fedorov AV (2017) Mathematical modeling of propagation of explosion waves and their effect on various objects. Combustion, Explosion and Shock Waves 53(4):433–443

Wang C, Qiu S, Eliasson V (2013) Quantitative Pressure Measurement of Shock Waves in Water Using a Schlieren-Based Visualization Technique. Experimental Techniques 40: 323–331

Zheng L, Lawlor B, Katko B, McGuire C, Zanteson J, Eliasson V (2020) Image processing and edge detection techniques to quantify shock wave dynamics experiments. Experimental Techniques – In review

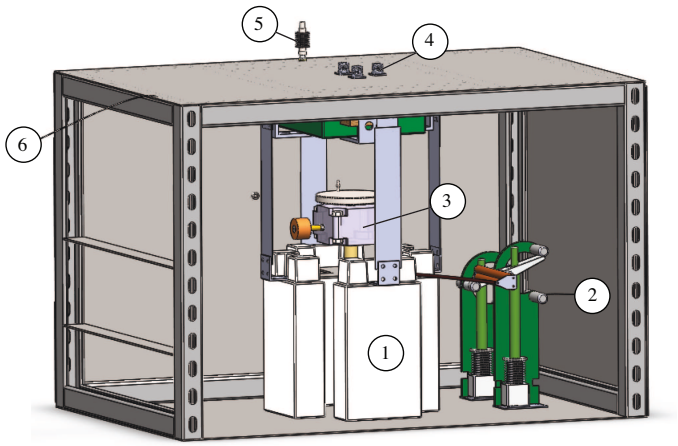

Fig. 1: The driver unit for the exploding wire setup: (1) four 10 kV capacitors, (2) electromagnetic switches, (3) spark gap, (4) electrode connector access ports coupled to the test section, (5) Rogowski coil, and (6) ground connection.

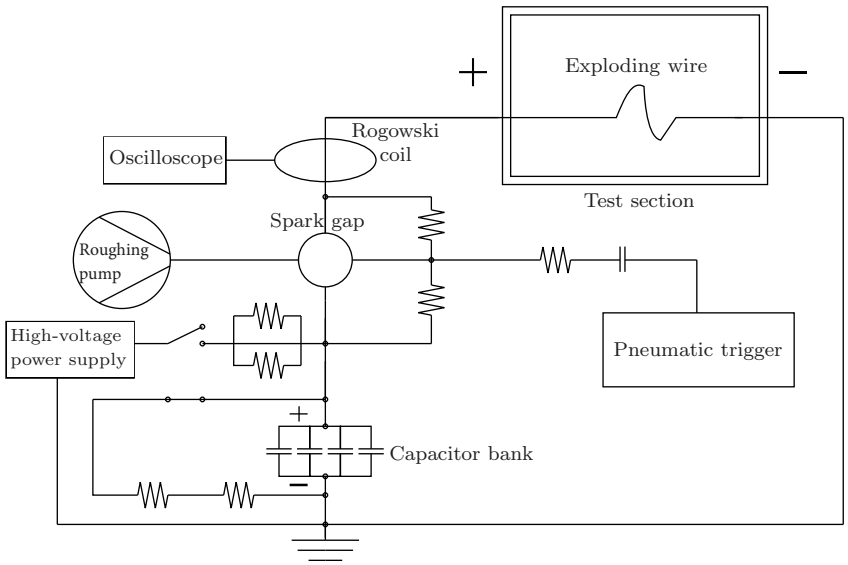

Fig. 2: The circuit diagram for the exploding wire setup shows how the overall experimental setup is connected.

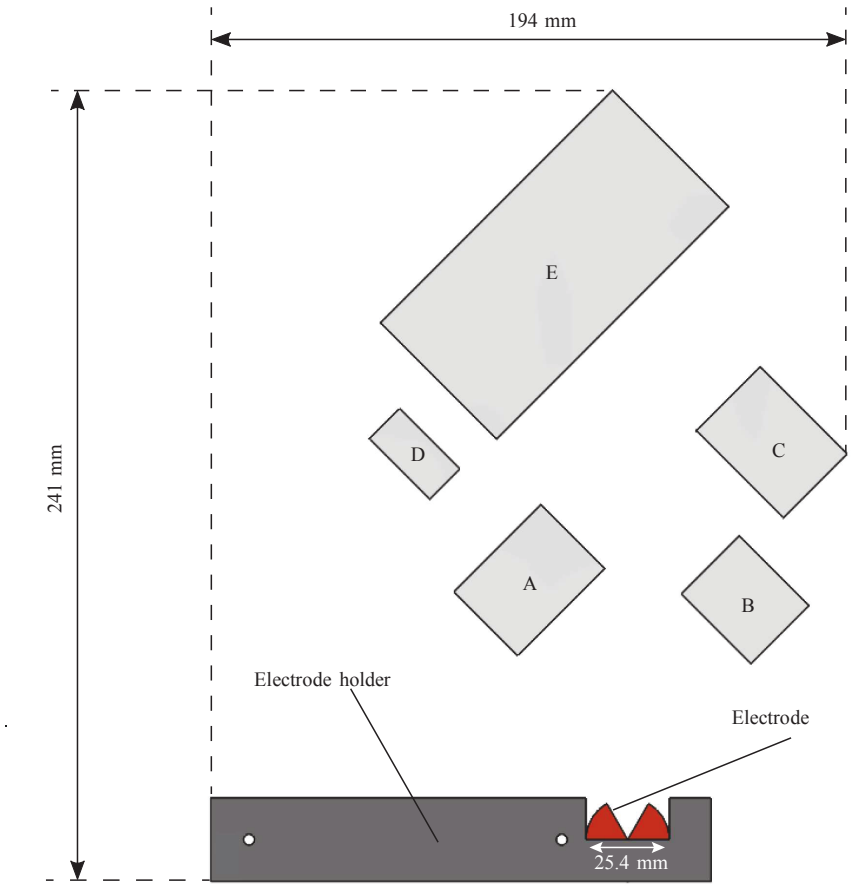

Fig. 3: Placement of structures A–E in relation to the exploding wire location.

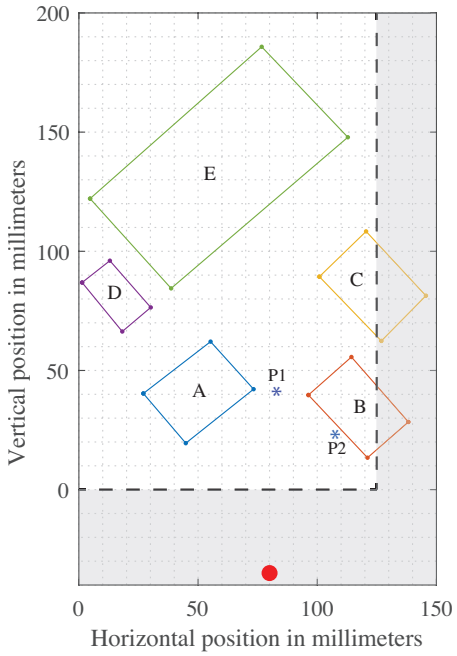

Fig. 4: Experimental test section arrangement showing obstacle placements and blast wave origin location (red circle). P1 and P2 correspond to two pressure probe locations used in the Overture simulations. Camera viewing area in white. Coordinate system shown in millimeters.

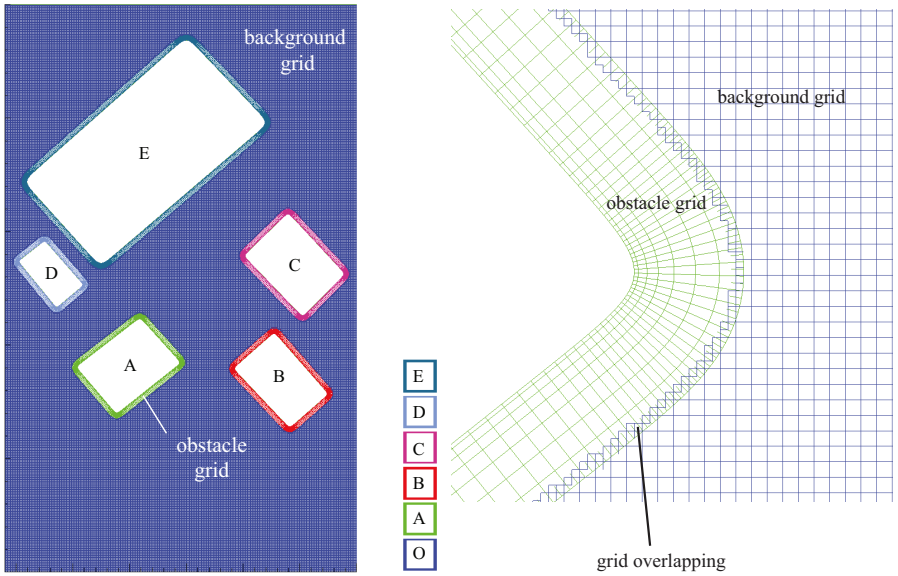

Fig. 5: Overlapping grid examples: (a) annular grids around structures A through E on top of a square background grid, and (b) overlapping grids between the background grid and the structures' grids.

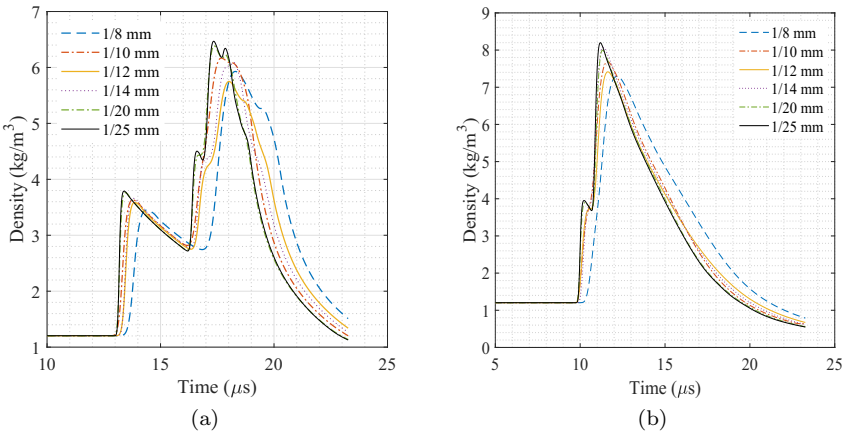

Fig. 6: Density results from using different grid sizes with the probe locations shown in Fig. 4: (a) density results from Probe 1 (P1 in Fig. 4) located between structures A and B, and, (b) density results from Probe 2 (P2 in Fig. 4) located 0.4 mm from structure B.

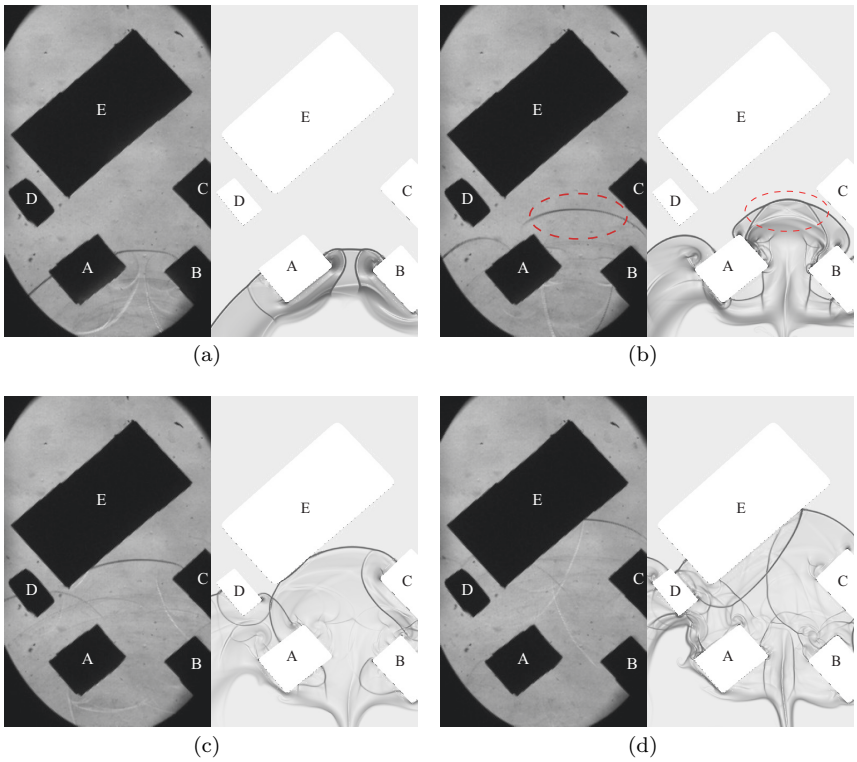

Fig. 7: Comparison of experimental (left) and numerical (right) schlieren results: (a) t = 16 µs, (b) t = 23 µs, (c) t = 31 µs,and (d) t = 38 µs.

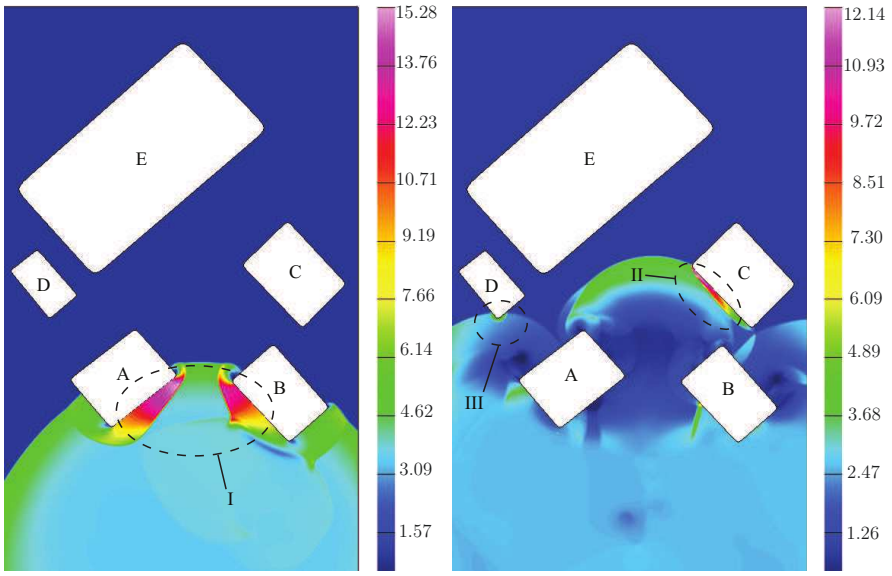

(a) t = 14.5 µs (b) t = 26.2 µs

Fig. 8: Nondimensionalized pressure contours at two time instants showing the resulting blast wave impact onto structures A and B.

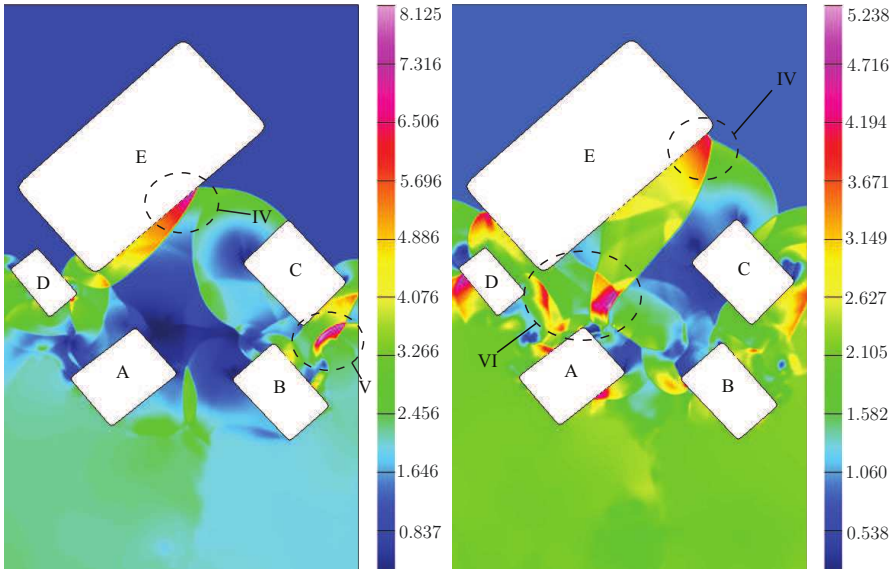

(a) t = 34.9 µs (b) t = 43.0 µs

Fig. 9: Nondimensionalized pressure contours at two later time instants showing the resulting blast wave impact onto all structures and the resulting shock-shock interaction in between the buildings.